

# Is the Jericho Escarpment a Tectonic or a Geomorphological Feature? Active Faulting and Paleoseismic Trenching

Michael Lazar, Zvi Ben-Avraham,<sup>1</sup> Zvi Garfunkel,<sup>2</sup> Naomi Porat,<sup>3</sup> and Shmuel Marco<sup>1</sup>

*Dr. Moses Strauss Department of Marine Geosciences, Charney School of  
Marine Sciences, University of Haifa, Haifa 31905, Israel  
(e-mail: lazar.michael@gmail.com)*

## ABSTRACT

The Jericho fault is considered to be the main active fault in the northern Dead Sea–lower Jordan Valley. In previous studies it has been identified by a prominent linear topographic escarpment that is thought to be the surface expression of this fault on land north of the Dead Sea. In this study, the paleoseismic natures of the escarpment and the fault were examined. Seismic activity was investigated in a series of three trenches excavated south of the fault trace on the surface. These trenches show evidence for Late Holocene faulting. A fourth trench excavated 300 m farther to the south exposed continuous, finely laminated marl from the ~80-ka Samra Formation at a depth of 2–0.6 m below the surface, with no evidence of faulting. This could suggest that the fault on land is segmented and that the nature of its activity changes from north to south toward the lake. Indeed, the continuation of this fault under the waters of the Dead Sea reveals active faulting along a sharp, segmented, linear bathymetric break, where the steep margin slope on the west meets the flat lake bottom. Evidence of drastic climatic changes and erosion are present in all trenches that were excavated, indicating that the prominent escarpment may in part be an erosional feature, perhaps formed by incision of an ancient Jordan River or along a Holocene lakeshore. A channel fill of a lacustrine nature that followed a period of erosion is interpreted as a high stand of the Dead Sea, which is contemporaneous with the Younger Dryas cooling period.

## Introduction

Field investigation of active faults depends on the ability to recognize their surface expression. In some cases expression is lacking, as faults do not always reach the surface. These faults can often be detected in paleoseismic trenches that are excavated to a few meters beneath the surface. In other instances, no surface or shallow subsurface expression may be detected. These are known as “blind faults” and are commonly limited to dip-slip motion in compressional environments (e.g., Somerville et al. 1996; Bakun and Hopper 2004). Linear escarpments and/or lineaments in young sediments are commonly interpreted as indications of active faulting (McCalpin 1996). One such fault, located north of the Dead Sea, is in part parallel to a linear

escarpment and is referred to as the Jericho (or Jordan) fault. This escarpment, which is clearly visible in air photos and satellite images, runs for about 10 km from north-northwest to south-southeast (trending 010°) and extends to the south, toward the northwestern corner of the Dead Sea, terminating approximately 2.5 km north of the present-day shore of the lake (fig. 1*b*). The cliffs, which are still well within the Dead Sea basin, are composed of laminated sediments of the Lisan Formation, the lacustrine formation deposited during the latest Pleistocene high stand of the Dead Sea.

The Dead Sea basin is situated along the Dead Sea fault system (also referred to as the Dead Sea rift or transform), a sinistral plate boundary separating the Arabian plate from the Sinai subplate (fig. 1*a*). The basin is bounded by two major strike-slip faults: the Arava fault at the southeast and the Jericho fault at the northwest (e.g., Garfunkel et al. 1981). Most of the recent tectonic activity in the northern Dead Sea basin has long been thought to

Manuscript received April 4, 2009; accepted January 19, 2010.

<sup>1</sup> Department of Geophysics and Planetary Sciences, Tel Aviv University, P.O. Box 39040, Ramat Aviv, Tel Aviv 69978, Israel.

<sup>2</sup> Institute of Earth Sciences, Hebrew University, Givat Ram, Jerusalem 91904, Israel.

<sup>3</sup> Geological Survey of Israel, 30 Malkhe Israel Street, Jerusalem 95501, Israel.

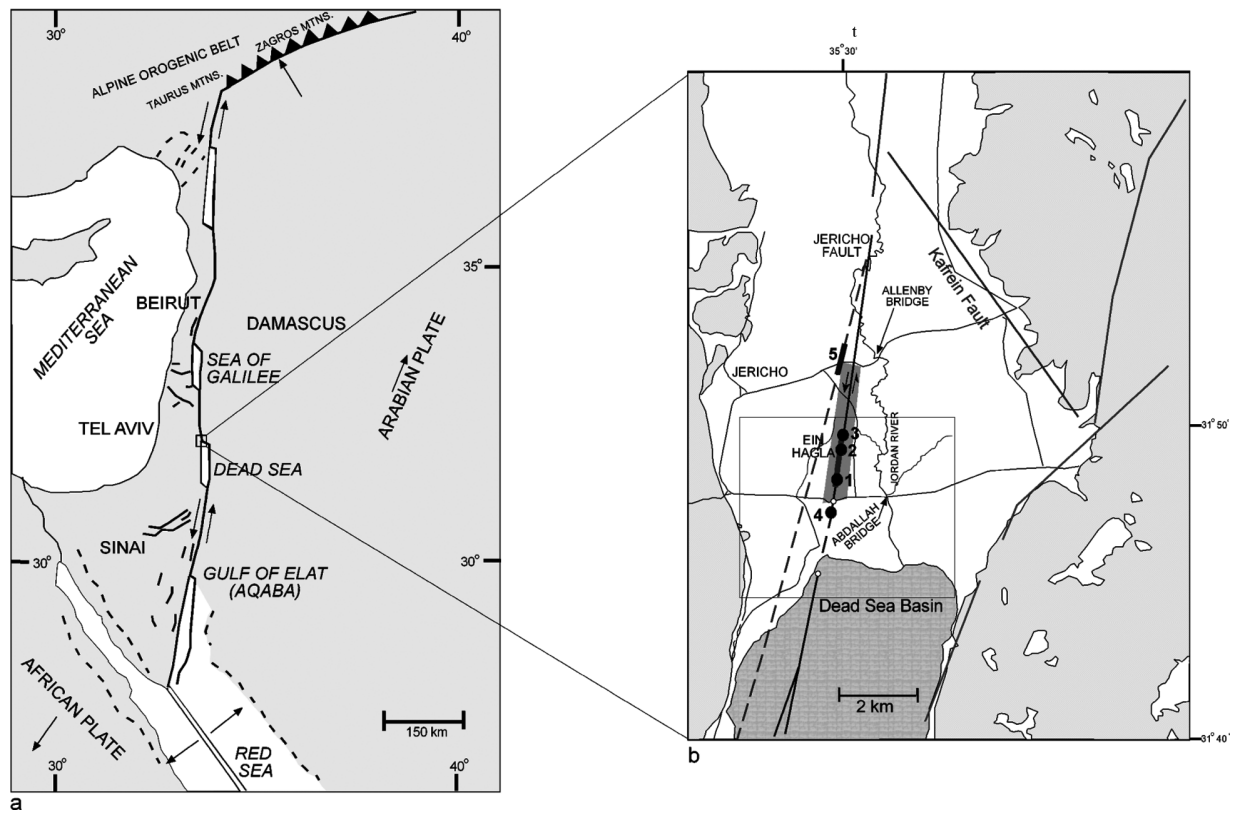


**Figure 1.** *a*, Tectonic setting of the northern Dead Sea area (following Ben-Avraham 1997). *b*, Location map of the study area showing the position of the Jericho escarpment (shaded gray area) and previous work performed in the area. Mapped and inferred faults in the northern Dead Sea basin–lower Jordan Valley showing Quennell (1959; long dashed line) and Reches and Hoexter (1981; thick dark line between locations 2 and 1). Documented field evidence on land is marked in thick solid lines: Begin’s (1974) observations are located at site 5, while those of Reches and Hoexter (1981) are at sites 1 and 2 and those of Gardosh et al. (1990) are at site 3. The thin black line indicating Reches and Hoexter’s (1981) observations more or less follows the eastern margin of the Jericho escarpment, which is not marked on the geological map (Sneh et al. 1998). On land, a small white circle marks the location of the fault observed in the roadcut, while location 4 marks the trenches investigated in the present study. The white circle on the fault in the lake marks the location of cracks observed on the floor of the lake during a manned submersible campaign (Lazar and Ben-Avraham 2002). The square outline indicates the area shown in figure 2.

occur along the Jericho fault (e.g., Garfunkel et al. 1981; Ben-Avraham 1997).

Exposures of lacustrine deposits indicate that the basin was occupied by several generations of lakes during the Pleistocene and the Holocene before it eventually desiccated to form the present Dead Sea. The two previous lakes deposited distinct and well-dated sediments (Zak 1967; Begin et al. 1974; Gardosh et al. 1990). The Samra Formation was deposited during the Middle-Late Pleistocene (U-Th age of  $\geq 80$  ka; Waldman et al. 2007). It is overlain by the Lisan Formation, which is U-Th-dated to be between 70 ka and 15 ka BP (Kaufman et al. 1992; Schramm et al. 2000).

Alternating seasonal laminas of evaporitic ara-

gonite and detritus, which accumulated at the bottoms of these lakes, are characteristic of both formations. They provide sensitive recorders of paleoseismic fault ruptures and fault activity (e.g., Marco and Agnon 1995). For this reason, it was assumed that signs of deformation (i.e., fault activity) in the Dead Sea area would be clearly evident in the sedimentary record of trenches excavated across the suspect fault in the area. Horizontal, undisturbed lamina would indicate lack of activity, since seismogenic faulting would leave its mark on these sensitive features.

The study area is located at the southern end of the morphotectonic depression known as the lower Jordan Valley. Here the valley, which is bordered

by large boundary faults, is about 25 km wide and possesses a southward slope of 1.7%. Surface sediments are mostly horizontal and consist mainly of coarse clastics and chinks of the Pleistocene Samra and Lisan Formations (Rotstein et al. 1991). The morphology of the area is hard to discern, as it has been modified for decades, first by the Dead Sea Potash Company and later by the military.

### The Jericho Fault

Two visual lines of evidence have been used to describe the Jericho fault. The first, a lineament that is clearly identifiable in air photos and satellite imagery of the lower Jordan Valley (fig. 2), has previously been interpreted as the surface expression of the Jericho Fault in this area, that is, the main active strand of the Dead Sea fault north of the lake (Quennell 1959; Begin 1974; Garfunkel et al. 1981; Reches and Hoexter 1981; Gardosh et al. 1990; Rotstein et al. 1991). This 15-km-long, ~10-m-high, 010°-trending row of cliffs is termed here the Jericho escarpment (or the Jericho Lineament; Shamir et al. 2005). The second line of evidence is a belt of considerable deformation that distorts the young sedimentary cover of the valley floor. This is the surface expression of a shallow fault, and it seems to partially follow the Jericho escarpment, where after about 3.5 km the two diverge by a few degrees. The fault can be followed until it is exposed in a roadcut along the road from Jericho to the Jordanian border (Abdallah Bridge; fig. 1*b*). In this area, the fault lies some 100 m to the east of the cliffs and can no longer be traced in the field farther to the south. Previous identification of the Jericho fault as the main active strike-slip fault in the area was based on field observations that are presented below and summarized in figure 1*b*.

**Surface/Shallow Subsurface Evidence.** The history of research along the Jericho fault is important in understanding why the Jericho escarpment was thought to be the surface expression of this fault and why this fault is thought to be the main strand of the strike-slip plate boundary in this area. The fault was first documented by Quennell (1959), who mapped it north of Jericho on the basis of an alignment of physiographic linear features and a line of fractures and flexures in young sediments along the valley floor (fig. 1*b*), an extremely unusual find in the Jordan Valley. The southern extension of the fault into the Dead Sea was inferred, although little information from the lake was available. Quennell (1959) interpreted this lineament as a strike-slip fault (fig. 1*b*, *long dashed line*) and was the first to

suggest the pull-apart model for the Dead Sea basin. Southward from Jericho, Quennell marked the fault as a dashed line—that is, concealed—to indicate that the fault has no surface expression in this area.

Begin (1974) mapped a section of the fault along the same alignment as Quennell where the Lisan Formation is deformed (location 5 in fig. 1*b*). In addition, he interpreted the Jericho escarpment as a 1.5-km-long normal fault.

Reches and Hoexter (1981) documented intense fracturing affecting young sediments ranging in age from 3500 BP to the present in trenches excavated across a lineament that is thought to be the southward continuation of the fault mapped by Quennell (locations 1 and 2 in fig. 1*b*). The authors correlated disturbed sediments found in the trenches to the catastrophic earthquakes of 31 BC and AD 749. Garfunkel (1981) concluded that the Jericho fault was a transpressional feature; this was later confirmed by Gardosh et al. (1990) and Rotstein et al. (1991). The former group documented small thrusts in trenches along the same lineament (location 3 in fig. 1*b*) close to the site examined by Reches and Hoexter, but they did not correlate the deformation with specific earthquakes. Gardosh et al. (1990) used the deformations they observed in the trenches north of the present study area to calculate a minimum slip rate along the Jericho fault of 0.7 mm yr<sup>-1</sup> for the past 3000–4000 yr. Unlike the previous studies, which focused on deformations in young sediments along the valley floor, Rotstein et al. (1991) examined deep seismic reflection data and suggested that the Jericho escarpment follows a major fault, that is, that it is the surface expression of the plate boundary in the area. However, limited seismic coverage and resolution (of the reflection data) and the proximity of this feature to the end of the seismic line raise questions as to the validity of this interpretation.

Recently, four high-resolution seismic reflection lines were acquired north of the lake (Shamir et al. 2005). Interpretation of these lines, according to the authors, indicates the presence of a fault at depth. However, the authors stress that the Jericho fault does not reach the surface, and they speculate that traces of recent activity observed in the field and in paleoseismic trenches are the result of salt diapirism and not neotectonics. They also attribute the formation of the Jericho escarpment to salt diapirism. In addition, Shamir et al. (2005) and Shamir (2006) indicate that activity along the Jericho fault, both on land and in the lake, ceased completely, presumably in the Late Pliocene or the Early Pleistocene, and that motion in the area is now spread

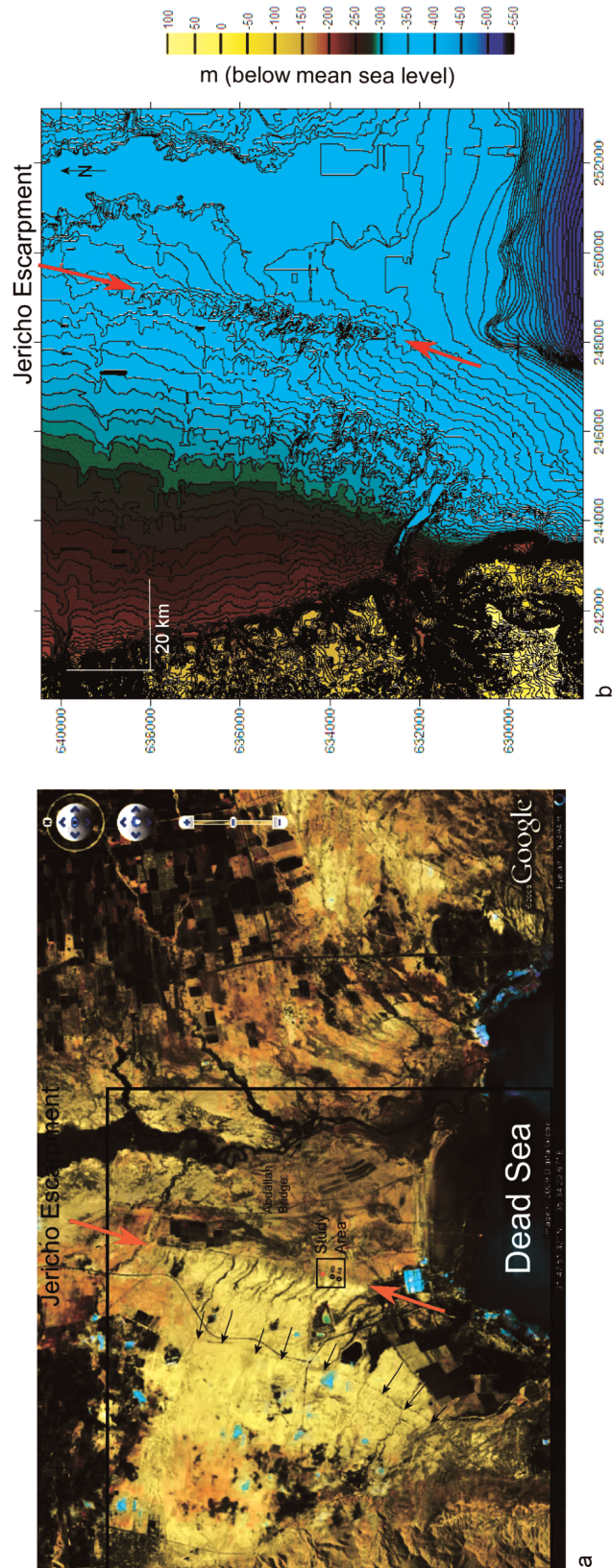


**Figure 2.** *a*, Northwestern shore of the northern Dead Sea (Google Earth mapping service, used with permission). The row of cliffs termed the Jericho escarpment is marked by red arrows. Small black arrows indicate an ancient shoreline that is more or less parallel to the escarpment. The study area is marked by a small square outline. A red circle marks the location of the fault observed along the road to the Abdallah Bridge. White circles mark the locations of trenches 4b and 4a in this study. The large square outline marks the location shown in *b*, which is the topographic map showing the Jericho escarpment (*red arrows*). Contours are every 10 m.

across a broad shear zone and not along a single fault.

The projected continuation of the Jericho fault trends southward into the waters of the Dead Sea, where it can be correlated with an underwater bathymetric scarp originally mapped with single-channel seismic reflection data (Neev and Hall 1979). The results indicated faulting in this area and led Garfunkel et al. (1981) and Reches and Hoexter (1981) to interpret the Jericho fault as a continuous feature extending from the western shoulder of the lake floor northward into the Jericho valley. However, since the expression of the fault along the transition from the land to the lake is unclear, it was either marked on some maps by a dashed line (e.g., Gardosh et al. 1990) or left blank (e.g., Garfunkel et al. 1981; Sneh et al. 1998). Several high-resolution seismic reflection studies (for a summary, see Ben-Avraham 1997), along with newer shallow seismic data (Lazar 2004) and observations from a manned submersible investigation (see fig. 1*b* for location) that included open cracks and fresh fault planes (Lazar and Ben-Avraham 2002), provided evidence for the recent and ongoing activity of the Jericho fault, at least in the lake and along its western margin.

In previous studies of the Jericho fault on land, significant strike-slip motion was inferred on the basis of several lines of deduction; the strong deformation of very young sediments without significant vertical offset of the floor of the Jordan Valley, the straight fault trace, and its assumed role as the border of a major pull-apart basin are all typical of a strike-slip fault. Moreover, lateral motion has been used to explain compressional features along its trace north of the Dead Sea (e.g., Garfunkel 1981; Rotstein et al. 1991) that are incompatible with normal fault slip. The Jericho fault is the only major known through-going fracture along the Jordan Valley that has the characteristics of a strike-slip fault. It was therefore the obvious candidate to take up the lateral motion along the Dead Sea fault, which is inferred from the offset of geologic features across the valley and from regional plate kinematics (e.g., Freund et al. 1970; Garfunkel 1981; Joffe and Garfunkel 1987). However, as stated, direct evidence for strike-slip motion across the southern extension of the fault trace or its assumed surface expression (the Jericho escarpment) is absent.

The lack in the proximity of the Jericho fault of useful markers that can be used to measure strike-slip movement across the Jericho escarpment, along with the desire to shed light on the transition of the Jericho fault from land into the Dead Sea,

were the motivation for the excavation of a series of trenches designed to examine the paleoseismic activity in the area. Two main questions regarding the surface expression of the fault arise. (1) Why is there no surface deformation along the entire fault, which is considered to be a major fault zone? That is, why is surface deformation absent in the segment south of the road to the Abdallah Bridge? (2) How was the topography of the Jericho escarpment produced, and how is it related to the fault? It is important to point out that conditions in the study area (from the northern shore of the Dead Sea to the road leading to the Abdallah Bridge; fig. 1*b*) are harsh and that it is a closed military zone. Therefore, access to the area is limited and additional studies and campaigns were not possible.

**Recent Activity of the Jericho Fault.** While the time frame covered by seismological data (instrumental) in the area is small (<60 yr) and the structural framework complex and the slip rate along the Dead Sea fault are not very high, earthquake focal mechanisms have nonetheless been used to describe motion in the area. These show a mixture of strike-slip, normal, and reverse movements (Ben-Menahem et al. 1976; van Eck and Hofstetter 1990; Rotstein et al. 1991; Shapira 1997; Shamir et al. 2005) and wide spatial distribution. While more recent studies do show predominately strike-slip faulting in the area (e.g., Hofstetter et al. 2007), it is impossible to conclude from these data alone that movement occurs today along a clear lineation or trend. On the basis of relocated epicenter distribution, Shamir et al. (2005) state that there is no evidence for distinct clustering of earthquake epicenters along the Jericho escarpment, and they use this, together with their interpretation of the newly collected seismic reflection data and lack of microseismicity, as evidence for the inactivity of the fault.

As a result of its assumed role as the major plate boundary in the area, the majority of current motion (coseismic and interseismic) is expected to occur along the Jericho fault. Hence, GPS measurements on local and regional scales should provide similar rates of tectonic motion. GPS measurements along the Dead Sea fault taken by Pe'eri et al. (2002) indicate a minimum slip rate of  $2.6 \pm 1.1$  mm yr<sup>-1</sup> for the entire fault during the time period from 1996 to 1999. Wdowinski et al. (2004) also used GPS measurements and calculated a higher rate of 2.8–3.8 mm yr<sup>-1</sup> for a period of 7 yr between 1996 and 2002. Both rates are significantly higher than the 0.7 mm yr<sup>-1</sup> (minimum) calculated by Gardosh et al. (1990) from offsets found in excavated trenches, but they are lower than the long-

term average of ca. 6 mm yr<sup>-1</sup> estimated by Joffe and Garfunkel (1987) on the basis of regional geology. More recently, Mahmoud et al. (2005) and Reilinger et al. (2006) calculated that left-lateral slip rates along the Dead Sea fault range from 4.4 ± 0.3 mm yr<sup>-1</sup> in the Gulf of Aqaba (southern Dead Sea fault) to 4.7 ± 0.4 mm yr<sup>-1</sup> in western Syria. Marco et al. (2005) investigated buried displaced stream channels and demonstrated that Late Holocene slip along the Dead Sea fault zone in northern Israel has primarily been strike-slip at a minimum rate of 3 mm yr<sup>-1</sup>. Assuming that the Jericho fault is the active plate boundary, some manifestation of this activity should be expressed along its trace.

### Trench Study

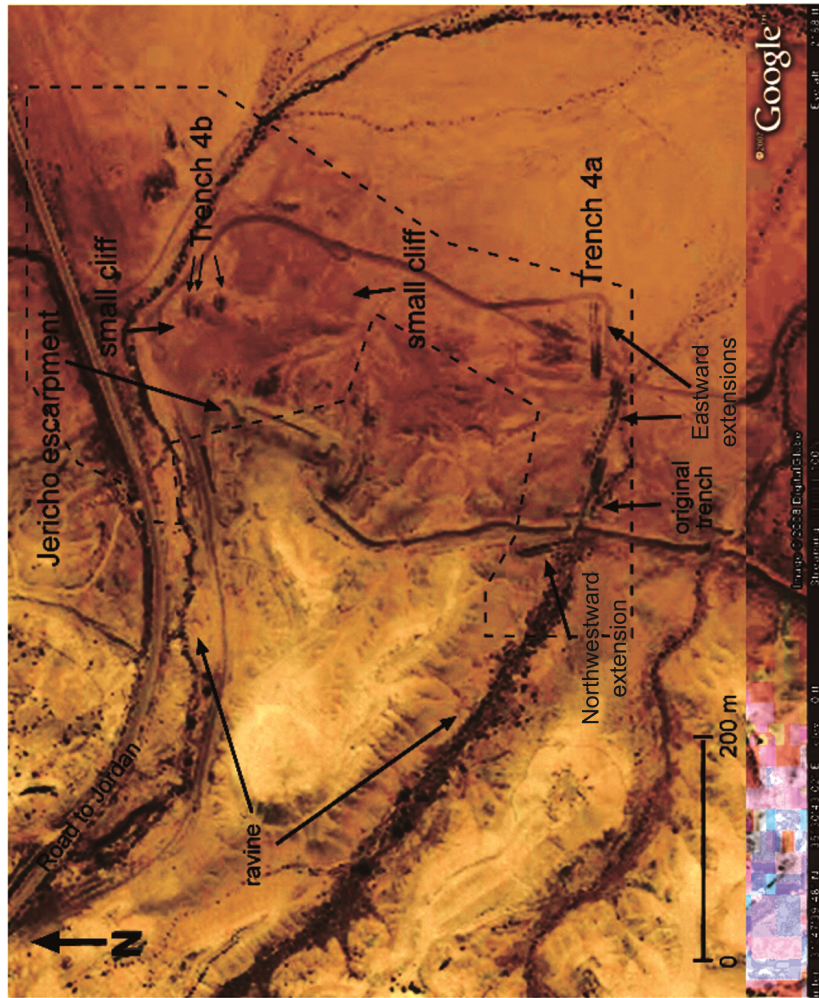
The Jericho fault is visible in a roadcut along the road leading to Jordan (fig. 1), but no surface evidence can be found farther to the south. In order to identify the Jericho fault in the area from the road to the shore of the Dead Sea, four east-west-trending trenches were excavated south of the previous studies, in three separate campaigns (location 4 in fig. 1*b* and trenches 4*a* and 4*b* in fig. 3). The first trench, trench 4*a* (the southernmost trench), was located along a small ravine that cuts into the hills and flows into the Jericho plain. It was excavated with the expectation of exposing recent alluvium from the ravine that had accumulated at the foot of the hills. The location was chosen in accordance with field relations, in line with the trend of the bathymetric escarpment in the lake and along the projected continuation of the fault observed and documented on land north of the study area. Field relations indicate that subsurface stratigraphy could be followed and traced under the Jericho escarpment (which lies some 100 m to the west)—that is, under the Lisan Formation—thus providing a clear age constraint on upper trench sediments. The trench was excavated to a depth of 3–4 m and a length of 100 m, a distance that spans the entire zone where the fault was expected. Evidence of faulting was not found in sediments exposed within the trench (fig. 4). This trench was later extended in a second campaign (fig. 3*a*) to assure that the fault had not been missed (see below). During the third campaign, three additional trenches were excavated some 300 m north of the initial trenching site (location 4 in fig. 1*b* and trench 4*b* in fig. 3) across a small topographic step that is possibly a fault-related feature. This scarp lies some 50 m to the east of the Jericho escarpment and is therefore probably not directly associated

with it. Trenches 4*b* (fig. 3) were located just south of where the surface trace of the fault was observed along the roadcut.

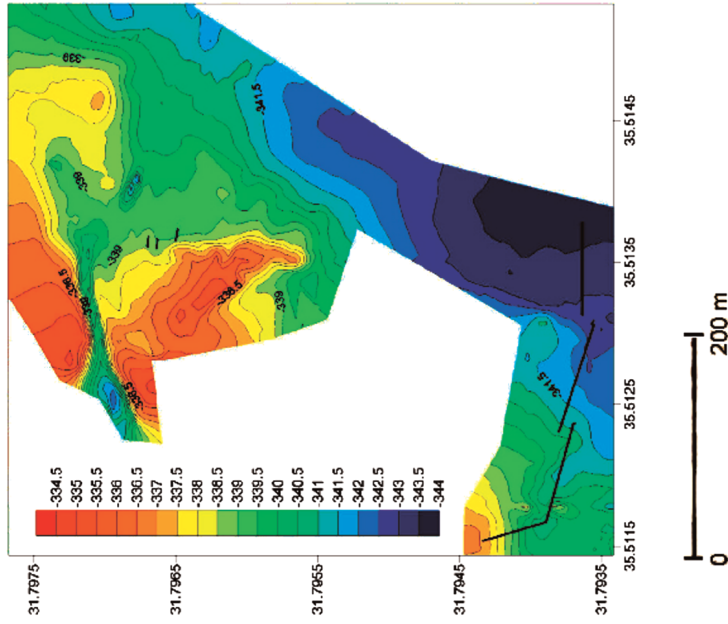
**Trench 4*a*: The Southernmost Trench.** Figure 4 presents the log of the central section (termed “original trench” in fig. 3*a*) of trench 4*a* (fig. 4*a*) and the schematic field relations observations (fig. 4*b*). Seven samples of organic matter were found and collected for <sup>14</sup>C dating (table 1; only six samples provided enough material for dating): three from the topmost (youngest) layer and two from the bottommost (oldest) layer. The log illustrates the uniformity of the layers exposed in the trench. The oldest unit to be uncovered, unit 1' (sample L1 located 2.7 m beneath the surface and dated outside the limit of radiocarbon resolution), consists of alternating horizontal laminas of aragonite and detritus. Unit 1' was followed westward undisturbed, through a northwest extension of the trench (fig. 3) and under the Jericho escarpment, that is, under unit 4 of the Lisan Formation. These field relations indicate that unit 1' belongs to the older, pre-Lisan Samra Formation (i.e., older than ~80 ka). Unit 1' is slightly tilted toward the east and vanishes toward the eastern end of the trench. Unit 2' is a sandy, <10-cm-thick layer, and unit 3 is massive shale dated to 13,025 ± 115 BP (sample L3: 0.9 m below the surface). Extension fractures (mode 1), which are mostly vertical with a main orientation of north-northwest (Shamir et al. 2005), are abundant in the shale. Many fractures are filled with crystalline gypsum and do not reach the bottom of the trench.

Near the west end of the trench, the density of the gypsum-filled fractures increases significantly in a 2–3-m-wide zone. However, unit 1' continues undisturbed below the fractures. For this reason the fractures are interpreted as desiccation cracks. Units 5' and 6' also postdate the deposition of the Lisan Formation. Unit 5' is the fill of two fossil stream channels that cut into the valley when Lake Lisan, the predecessor of the Dead Sea, dried up. The channel observed at the northern face of the trench is higher than that observed in the south face, indicating southward flow. Unit 6' (samples C1–C3, <sup>14</sup>C dated to post-1950) is a thin veneer of alluvial sand that covers the whole plain, thinning westward toward the hills and unconformably overlying units 3 and 5' (fig. 4).

The Lisan Formation (unit 4) is eroded and absent from the trench. None of the layers observed were offset or disturbed, and faults were not detected. In order to assure that the fault was not missed due to insufficient coverage to the east, a second campaign focused on extending the trench by another



a



b

**Figure 3.** a, Study area (Google Earth mapping service, used with permission) showing location of trenches and field relations between the Jericho escarpment and the small cliff discussed in the text. The dashed contour marks the area of topographic map shown in b, which is the topographic map of the small cliff showing location of trenches. Contours are in meters below sea level.

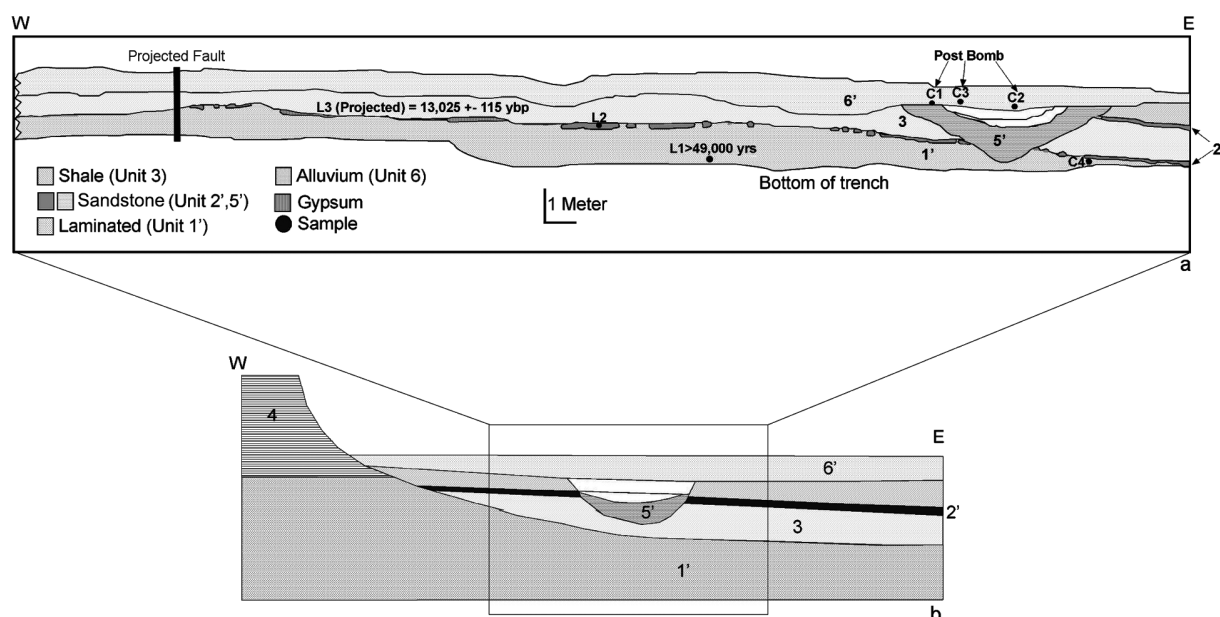


**Figure 4.** *a*, Log of the central section of the southernmost trench (trench 4a), with radiocarbon ages. The area documented in this log is marked "original trench" in figure 3a. The oldest exposed layer (>49,000 BP) is composed of unfaulted lamina. C1, C2, and C3 were dated postbomb (ca. 1950, when atmospheric testing of atomic bombs began), as was C4 (probably the intrusion of a root). Sample L2 did not contain enough organic material for dating. The location where the fault was expected according to field relations is marked "Projected Fault." Note that the westward extension of the trench is not shown in the figure, given its similarity to the section already shown. *b*, Schematic field relations according to trench observations.

50 m eastward. The continuation was a little shallower than the original trench. As in the original trench, undisturbed laminated layers (unit 1') were encountered within this unit that could be followed for the entire length of the trench, indicating that no near-surface faulting has occurred there in the past ~80 ka.

**Trenches 4b: The Northern Trenches.** The trench logs and schematic field relations for the northern trenches (location 4b in fig. 3) are presented in figure 5. Due to total lack of organic material, optically stimulated luminescence (OSL) dating was used to date significant events. The ages are presented in table 2. Evidence for Holocene faulting was found in all three trenches (fig. 6). As with the southern trench (location 4a, fig. 3), evidence for a southward-flowing stream or gully was found (unit 4, fig. 5), but general stratigraphy differs significantly. The sediments in these three trenches are indicative of a subaerial environment rather than a lacustrine one. Deformation included offset layers, fractures, and fissures. Dip angles of the observed fault strands were very steep, nearly vertical. Strike slip may have been accommodated along

these faults, although stratigraphy did not provide solid constraint for its measure. A main fissure-like fault was apparent in all the trenches and was filled with very deformed material of an origin that could not be determined. However, in the southern face of the middle trench, a few distinct shear planes were uncovered, overlain by unit 6. In total, pre-unit 6 vertical throw was approximated at 1 m on average. Except for the main fault, it is hard to correlate the fault strands on both faces of the trench. This probably indicates that they are short, perhaps en-echelon, secondary features that accompany the main strand.

The sedimentary units uncovered in the northern trenches (4b) are younger than ~3000 yr (table 2). This is significantly different than the ages of units found in the southernmost trench (4a), despite the close proximity of the two areas and similar topographic levels. In addition, the depositional environments seem to greatly differ: the sediments of the southernmost trench were deposited in a lacustrine environment, while the northern trenches contain mainly alluvial and sabkha sediments. This could be explained by the northern sediments being

**Table 1.** Radiocarbon Ages for Samples Collected in Trench 4a (Southern Trench)

ID	No.	Type	Pmc $\pm 1\sigma$	$^{14}\text{C}$ age $\pm 1\sigma$ BP	Calibrated age BP	$\delta^{13}\text{C}$ ‰ PDB
C1	3951	Charcoal	150.3 $\pm$ 1.0	Postbomb	...	-23.5
C2	3952	Plant	124.0 $\pm$ .7	Postbomb	...	...
C3	3953	Charcoal	161.4 $\pm$ 1.1	Postbomb	...	-25.27
C4	3954	Charcoal	108.3 $\pm$ .7	Postbomb	...	-20.9
L1	3955	Plant	...	>49,000	...	-29.1
L3	3956	Plant	25.5 $\pm$ .3	10,975 $\pm$ 80	13,025 $\pm$ 115	-22.4

Note. Pmc = percent modern carbon. Analysis and calibration were performed by the Radiocarbon Dating Laboratory, Department of Environmental Sciences and Energy Research, Weizmann Institute of Science, Rehovot, Israel. Calibrations follow those by Stuiver et al. (1998).

deposited in a preexisting relief and subsequently eroded, probably in connection with faulting or incision of a river (possibly the Jordan).

In all three northern trenches (4b), sedimentary units from one side of the fault zone to the other could not be matched within the same trench. This may be explained in part by the presence of the fault-parallel channel found in the form of coarser, white sand (unit 4a, fig. 5) on the eastern side of the trenches that would have eroded existing sediments, making correlation difficult if not impossible.

Evidence of at least two faulting events was found in all the northern trenches (fig. 5). This included faults and displaced and discontinuous layers that could not be correlated from one side of the trench to the other. The earlier offset postdates unit 2 and predates unit 3. This is expressed by the upward terminations of faults on both faces of the northern trench. The latest fault ruptures through unit 5 and predates unit 6. In terms of ages, unit 6 is dated by samples BAF-6 and BAF-2 to  $430 \pm 40$  and  $1640 \pm 180$  BP, respectively. However, two problems arise as a result of this dating: first, BAF-5 is younger than the overlying BAF-3, and second, BAF-4 is younger than the overlying BAF-2. If the date of  $1130 \pm 70$  BP obtained for BAF-4 is correct, then the last rupture postdates  $870 \pm 70$  CE and the dating of BAF-2 is erroneous. If the date for BAF-4 is wrong and that for BAF-2 is correct, in which case the last rupture predates  $360 \pm 180$  CE, then the event could be associated with either the 31 BCE or the 363 BCE earthquake. The earlier event, which postdates unit 2 and predates unit 3, remains undated because of the fact that BAF-3 from unit 3 is dated as 3400 BP while BAF-5 from unit 2 is dated as 2600 BP. Since it is impossible to know which of these dates are wrong, the large uncertainty prevents assigning absolute ages to the faulting events.

Together with the southern trench (trench 4a, fig. 3), observations indicate that the last strong earth-

quake in the area, the magnitude 6.2 1927 Jericho earthquake, did not cause rupturing at all along this segment (Shapira et al. 1993) or produce surface deformation in the vicinity of the trenches, although extensive damage was reported in the nearby city of Jericho (for a critical assessment of this damage, see Avni et al. 2002). This is consistent with the findings of Reches and Hoexter (1981) and Gardosh et al. (1990), who also did not report finding any indications for this event, and it is inconsistent with the theory that this fault accommodates all the motion in the area. It would also seem, given the date of unit 6 (BAF-4, table 2) in the northernmost trench (fig. 5), that this part of the Jericho fault has not ruptured for at least 1000 yr. This is in keeping with the conclusions of Shamir et al. (2005) and Shamir (2006). However, they claim that the fault has been inactive for a much longer period of time (at least 1.8 Ma), while findings from the northern trenches presented in this study show evidence of Holocene activity.

## Discussion

The observed sequence in trench 4a (southern trench) represents the following geological history: after deposition of the lacustrine Samra Formation (unit 1'), the younger Lisan Formation accumulated during the last glacial period. Aerial exposure led to erosion of part of the Jericho plain when lake levels dropped. Extensive erosion of the Lisan Formation is well known from other areas along the Dead Sea. As water levels began to rise again, unit 3 (shale) was deposited. The absence of carbonate lamina—that is, the absence of a seasonal signature—indicates that the water in this location did not reach saturation during summer. A layer of sand at the top of unit 3 indicates a drop in lake levels and an additional low stand, while fractures formed at the surface as a result of desiccation. Erosion and incision set in, after which unit 5' (stream fill) was deposited. The fossil streams flowed south-

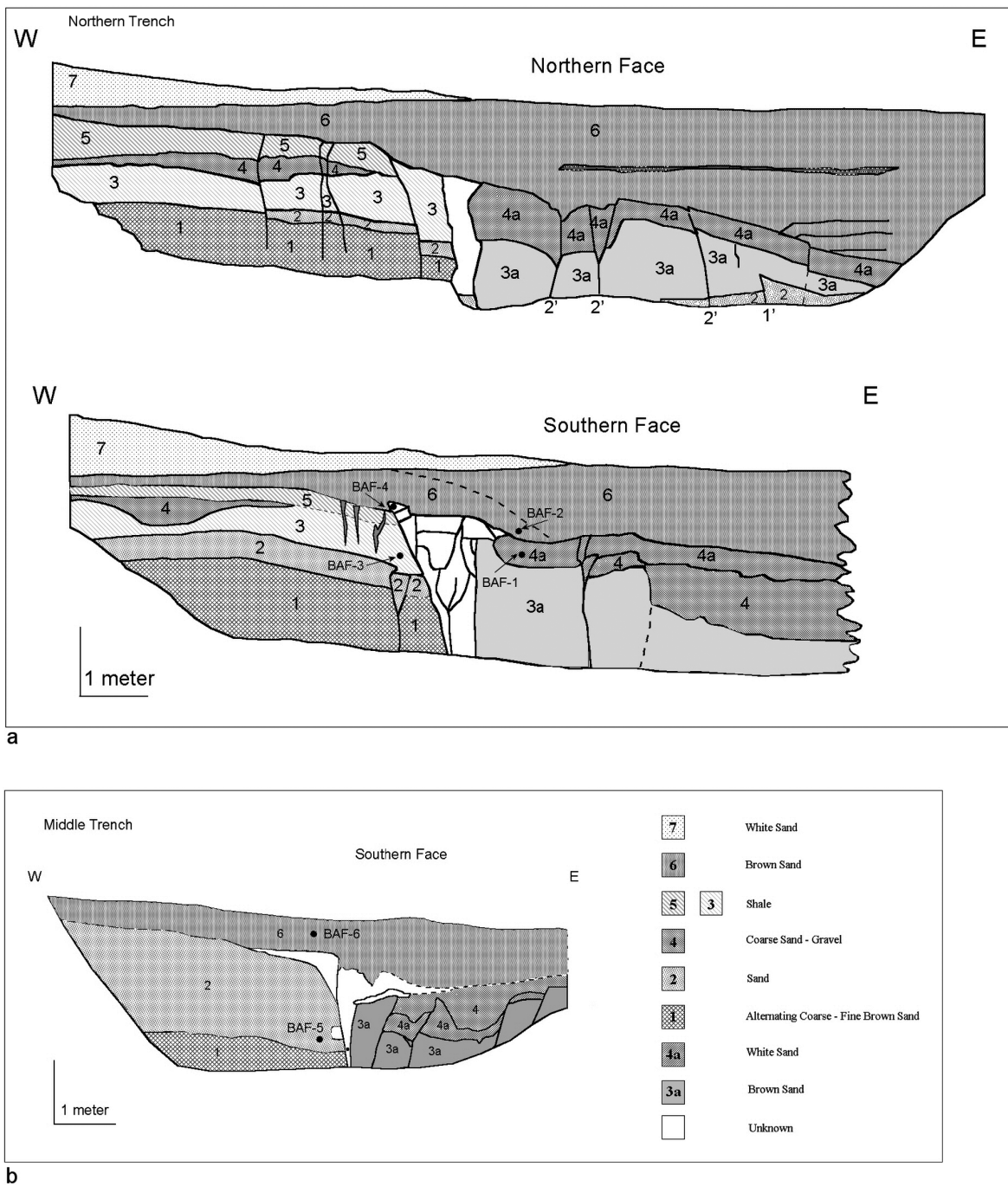


**Figure 5.** Logs of the northern trenches 4b and sample locations BAF 1–6. Luminescence ages are presented in table 2. *a*, The northernmost trench, northern face and southern face of the trench. Evidence of two seismic episodes can be deduced from the northern face (see locations on fig. 2). *b*, Southern face of the middle trench.

ward and incised into the shale layer (unit 3) to a depth of at least 2 m. An additional phase of erosion took place, and finally unit 6' (alluvial and eolian cover) was deposited.

During the Pleistocene, the Samra Formation

was deposited in a lake, hence the laminated character of unit 1' in the southern trench (trench 4a). The absence of the Lisan Formation in the northern trenches (trenches 4b) indicates that after its deposition, erosion occurred, perhaps aided by the

**Table 2.** Field and Laboratory Data for Optically Stimulated Luminescence (OSL) Ages

Sample ID	Location	Depth (m)	Field $\gamma$ ( $\mu\text{Gy yr}^{-1}$ )	K (%)	U (ppm)	Th (ppm)	External $\alpha$ ( $\mu\text{Gy yr}^{-1}$ )	External $\beta$ ( $\mu\text{Gy yr}^{-1}$ )	Total dose ( $\mu\text{Gy yr}^{-1}$ )	No. disks	De (Gy)	Age (yr)
Northern trench, south wall:												
BAF-1	Remain faulting	1.5	740	.20	1.38	1.07	4	329	1074 $\pm$ 77	8/16	3.09 $\pm$ .44	2900 $\pm$ 460
BAF-2	Early postfaulting	1.25	849	.65	2.62	2.76	9	822	1680 $\pm$ 90	10/17	2.75 $\pm$ .27	1640 $\pm$ 180
BAF-3	Fill of fracture	1.4	877	.89	2.76	3.04	10	1005	1892 $\pm$ 94	9/13	6.43 $\pm$ .54	3400 $\pm$ 330
BAF-4	Postfaulting	.9	746	.76	3.28	2.53	11	971	1728 $\pm$ 61	10/12	1.96 $\pm$ .09	1130 $\pm$ 70
Central trench:												
BAF-5	Early postfaulting	1.4	991	.90	2.29	3.22	8	958	1957 $\pm$ 104	5/12	5.09 $\pm$ .25	2600 $\pm$ 190
BAF-6	Youngest truncation	.4	1189	.96	3.03	4.29	11	1114	2314 $\pm$ 124	9/12	.99 $\pm$ .08	430 $\pm$ 40

Note. Measurements were performed on quartz samples with grain sizes of 88–125  $\mu\text{m}$ , etched with concentrated HF for 40 min. The equivalent dose (De) was obtained using the single-aliquot regenerative dose (SAR) protocol and the OSL signal, using preheats of 10 s at 220°–260°C. All samples show good preheat plateaus, recycling ratios within 5% of 1.0, and no infrared signals. Most dose distributions are skewed toward older values. Water contents were estimated at 5%  $\pm$  2%. Field  $\gamma$  was measured in situ using a portable gamma scintillator. K, Th, and U concentrations in the sediment were measured using inductively coupled plasma mass spectrometry. These concentrations were used to calculate the external  $\alpha$  and  $\beta$  dose rates. Total dose is the annual dose rate to the sample (in microgrey per year). No. disks is the number from those measured that was used for calculating the De.

paleo-Jordan River. However, during the Holocene lake level high stand, river flow was greatly reduced, once again allowing for sedimentation. These sediments were probably deposited under disturbed conditions (or the flow of freshwater from a river or stream), which prevented the formation of laminae and produced the homogeneous massive shale of unit 3.

The location of the small escarpment in the northern study area (fig. 3) is probably associated with the faults observed in the northern trenches (trenches 4b, fig. 3) but not with the Jericho escarpment, which lies >50 m to the west. This observation, together with a lack of faulting in the southernmost trench across the southern projection of the Jericho escarpment (trench 4a, fig. 3) and a lack of evidence in the field for faulting at the base of the escarpment, led to the conclusion that while north of the study area this prominent topographical lineament may be associated with the Jericho fault, toward the study area the two features diverge and there is no direct connection between them. The formation of the Jericho escarpment postdates the deposition of the Lisan Formation, but in the southern trenches, continuous layers of the older Samra Formation are not faulted. Faulting in the northern trenches is in line with the trace of the Jericho fault, as detected in previous studies (fig. 1b; e.g., Reches and Hoexter 1981) and in the field. However, the possibility that the cliff initially formed in connection with the fault and then retreated westward as a result of erosion or wave action during a Late Pleistocene–Holocene lake high stand may explain the deviation of the fault with respect to the Jericho escarpment but not its seemingly segmented behavior. The possibility that the

Jericho fault is a blind strike-slip fault not reaching the surface but actively deforming it (and hence that it is responsible for the formation of the Jericho escarpment) is less likely, as blind strike-slip faults are extremely rare (Talebian et al. 2004). According to the trend of the fault interpreted in high-resolution seismic profiles (Shamir et al. 2005; Shamir 2006), the fault at depth would thrust toward the west. The hanging wall would be thrust westward, forming a westward-facing scarp or monocline and not the eastward-facing Jericho escarpment. In any case, the escarpment is probably not the direct result of displacement of the land surface by a fault, as previously suggested, but instead it is an erosive post-Lisan feature, as indicated by the lack of evidence for such a fault in the southern trench.

Surface rupture associated with historical earthquakes is common along the Dead Sea fault (e.g., Amit et al. 1995; Bowman 1995; Marco et al. 1997; Klinger et al. 2000; Zilberman et al. 2005; Ferry et al. 2007). In light of the above results, three questions must be addressed: (1) Where is the Holocene slip accommodated in the northern Dead Sea area? (2) How can the absence of faulting in the southernmost trenches (trenches 4a) be explained in light of evidence for rupture 300 m to the north (trenches 4b)? And (3) how was the Jericho escarpment formed?

As for the first question, continuous unfaulted layers of the Lisan Formation are exposed in the ravines west of the cliff. Therefore, the main strike-slip fault zone was thought to lie to the east of the cliff. North of the study area, the Jericho escarpment lies in the proximity of the fault zone investigated by Reches and Hoexter (1981; locations 1 and 2 in fig. 1b). However, in the study area the



**Figure 6.** Aerial photo of the middle trench: the northern face (log not presented in fig. 5), showing a fault that offsets a layer of coarse sand, probably layer 4a.

escarpment diverges from the trace of the fault toward the south and lies some 40–50 m to the west of the surface expression of the fault (expressed in the northern study area by the small topographic slope seen in fig. 3*b*, and not by the Jericho escarpment as previously thought). Southward of the three trenches, all field evidence vanishes and the fault does not pass through the southernmost trench (trench 4a).

The Jericho fault is visible in the northern trenches that were excavated for this study (trenches 4b), which offset layers dated to ~3000 BP, but it is absent in the southern trench, at least in sediments younger than 49,000 BP. One explanation for this observation is that the fault may be segmented. Fault termination, segmentation, and step-over have been shown in numerous models and are well documented along actual ruptures of active faults, where one “segment” has stopped and motion has been taken over by a neighboring one (e.g., Sieh 1996).

The importance of segmentation in controlling the development of topography in strike- and oblique-slip fault systems has been the focus of many recent studies (for a summary, see Booth-Rea et al. 2004). It is well recognized that displacement in oblique-slip systems generates topographic gradients (uplift being associated with antidualational jogs). Evidence for segmentation along the Dead Sea fault has been presented in the past by Garfunkel et al. (1981) for a number of areas and by Zak and Freund (1966) for the southern Arava valley. Seg-

mentation in the study area could be evidence of deeper structural control and could result from a change in direction of the plate boundary. According to Rotstein et al. (1991), the existence of a buried monocline south of Jericho is direct evidence of compression resulting from a change in direction of the main strike-slip fault (local right jog in the left-lateral master strike-slip fault). Evidence presented in this trenching study suggests that this change in the stress regime is also reflected in the shallow subsurface by lack of evidence for faulting in the southern trenches, that is, by segmentation.

In addition, this proposed pattern of segmentation is similar to the shallow fault pattern observed in the lake itself (e.g., Ben-Avraham et al. 1993; Ben-Avraham 1997; Lazar 2004). Segmentation would also explain the conclusions of Shamir et al. (2005) and Shamir (2006) that the Jericho fault has not been active since at least the Early Pleistocene: the seismic profiles examined in their studies are located in the southern area mapped in the current study, where no surface evidence of the fault was found (i.e., along the inactive fault segment). Farther to the north, activity resumes along the trace that is mapped and dated in the northern trenches. While on a much smaller timescale, this is also in keeping with earthquake focal mechanisms and microseismicity results (e.g., Rotstein et al. 1991; Shamir et al. 2005; Shamir 2006; Hofstetter et al. 2007) that indicate activity in the lake, lack of activity in the study area, and resumption of activity farther to the north. Although the Bouguer gravity

map does in fact indicate a sharp gravity gradient suggesting the presence of a deep-rooted basin boundary in the area (e.g., ten Brink et al. 1998), the resolution is too poor to resolve the issue of segmentation.

The possibility that the Jericho escarpment was formed by geomorphic or nontectonic processes (e.g., wave action) must be addressed. For this, a considerable drop in lake level is required. Initially, the level of the lake would have had to be higher than the present-day topography to allow for the deposition of the lacustrine sediments that compose the Jericho escarpment (the Lisan Formation). Significant fluctuations in the range of tens to hundreds of meters are known from analysis of Dead Sea lake levels (e.g., Bartov et al. 2003). Dropping lake levels would allow streams (such as the one found in trenches 4a and 4b) to flow, creating a pair of semiparallel cliffs, one on each side of the valley. According to Bartov et al. (2003), lake levels began to drop steadily from an extreme high stand of 160 m below mean sea level (MSL) around 25 ka to 330 m below MSL around 15 ka (the lower limit of their study) and continuing to drop. The lake almost totally desiccated either between 15 and 10 ka (Neev and Hall 1979) or between 11 and 8.5 ka (Yeichieli et al. 1993), and at some point its level was equal to the current topography at the base of the cliff (at -375 m; thus allowing for wave-cut action). Signs of this desiccation are evident in the trenches (see below). The Jericho plain in the study area lies at 350 m below MSL and represents a well-known erosional unconformity between the Lisan Formation and an overlying lacustrine unit (M. Stein, personal communication, 2001). This indicates that the conditions for massive erosion probably existed at some time during the last 15,000 yr. Bartov et al. (2003) showed that a previous lake level corresponded exactly with the Jericho escarpment. In addition, remains of ancient shorelines subparallel to the escarpment were identified farther to the west (Begin 1974). The Jericho escarpment follows the trend of these shorelines (fig. 2). These findings lend support to the assumption that this is a geomorphologic feature rather than a tectonic one, but they do not explain the proximity of the cliff to a previously active fault.

Another possibility of the formation of the Jericho escarpment was put forth by Shamir et al. (2005). According to their theory, salt diapirism in the area caused the uplift, the normal faulting, and the surface deformation observed along the length of the escarpment. However, no evidence for diapirism was found in the comprehensive seismic study performed by Lazar et al. (2006). In addition,

as the authors suggest, a salt diapir rising from a basin located east of the fault would create a west-facing cliff and not the east-facing Jericho escarpment.

**Climatic Implications.** Within the trenches, local environmental changes are expressed by the type of deposited sediment. Alternations of shale and sand were interpreted in this study as reflecting high and low lake-stand environments, respectively. Hence, the two layers of sand in trench 4a (unit 2, fig. 5) represent periods when Lake Lisan was drying out. Shale (units 1' and 3) is indicative of a lacustrine environment. The upper shale unit (unit 3) dates to  $13,025 \pm 115$  BP and seems to correspond to an Early Holocene high-stand episode preceding the almost total desiccation of the lake (Neev and Hall 1979; Yeichieli et al. 1993; Bartov et al. 2003). Stein (2001) notes that "the time interval ~14–11 ka is not represented in the sections or drill holes studied so far" (p. 278) in the Dead Sea, south of the present study area, but our finding may indicate that while the lake was drying out, a number of small ponds or lagoons were left behind and continued to receive a constant supply of sediments.

Evidence of a more humid period that occurred 13,000 BP was also found farther south in the Negev desert (Goodfriend and Magaritz 1988), indicating a savannah landscape. Unit 3 from the southern trench (trench 4a, fig. 3), which falls in this date range, could also correlate to a high stand of the lake, as evidenced by halite crystals uncovered in boreholes farther south near Ein Gedi and dated to the same period (Yeichieli et al. 1993). Unit 3 is overlain by a layer of sand (unit 2', fig. 4) that could correspond to the erosional period seen to the south before 11,315 BP (Yeichieli et al. 1993). During the subsequent dry spell, lake levels dropped significantly enough to allow a small stream to flow into the valley toward the Dead Sea. However, lake levels rose again, as can be seen by the deposition of lacustrine shale within the stream channels (unit 5'). The age of this high stand is constrained by unit 3 and unit 6'. It is, therefore, younger than 13 ka and older than postbomb (ca. 1950, when atmospheric testing of atomic bombs began). As no other evidence exists for significant lake-level rises during this period (e.g., Bartov et al. 2003), unit 5' is interpreted as indication of the Younger Dryas, a period of cooling that occurred during the warming trend to the current interglacial period and ended at about 12 ka. The Younger Dryas lasted ~1000 yr and led to enormous but short-lived changes in the climate of northern Europe (Broecker et al. 1988). The results presented here could provide direct evi-

dence for the Younger Dryas event in the eastern Mediterranean and the resulting environmental changes.

### Conclusions

Results of this study demonstrate the problems involved with the correlation between geomorphologic and tectonic elements, particularly in areas that are sensitive to climatic changes, such as Quaternary lake shores. Great care should be taken when interpreting linear escarpments as representing surface rupture or active fault scarps or when interpreting surface deformation as direct evidence for current activity. A paleoseismic trench study and geomorphic analyses indicate that the interpretation of the Jericho fault north of the northern Dead Sea shore as a continuous, recently active main tectonic element may not be as straightforward as previously thought. Results of this study show that while part of this area was active during the Holocene (northern trenching sites), other sections that lie along the projected continuation of

the same fault line (southern trench) were not. In order to directly connect the fault zone on land with the proven activity of the bathymetric cliff in the lake, absence of activity during the last 80,000 yr from the southernmost trench needs to be resolved. This can be resolved by assuming that the fault zone in the lower Jordan Valley is segmented. This is similar to the picture obtained for the shallow faults in the lake (Ben-Avraham et al. 1993). Questions still remain as to how strike-slip motion in the Jordan Valley is accommodated by primarily normal faulting around the Dead Sea basin and into the lake, as well as to the exact origin of the Jericho escarpment, that is, tectonic, geomorphologic, or both.

### ACKNOWLEDGMENTS

We would like to thank A. M. Michetti and an anonymous reviewer for their constructive comments, as well as L. Lev, N. Wechsler, and U. Schattner for their help with the fieldwork.

### REFERENCES CITED

- Amit, R.; Harrison, J. B. J.; and Enzel, Y. 1995. Use of soil and colluvial deposits in analyzing tectonic events: the southern Arava Rift, Israel. *Geomorphology* 12:91–107.
- Avni, R.; Bowman, D.; Shapira, A.; and Nur, A. 2002. Erroneous interpretation of historical documents related to the epicentre of the 1927 Jericho earthquake in the Holy Land. *J. Seismol.* 6:469–476.
- Bakun, W. H., and Hopper, M. G. 2004. Magnitudes and locations of the 1811–1812 New Madrid, Missouri, and the 1886 Charleston, South Carolina, earthquakes. *Bull. Seismol. Soc. Am.* 94:64–75.
- Bartov, Y.; Goldstein, S. L.; Stein, M.; and Enzel, Y. 2003. Catastrophic arid episodes in the Eastern Mediterranean linked with the North Atlantic Heinrich events. *Geology* 31:439–442.
- Begin, Z. B. 1974. The geological map of Israel, Jericho sheet (with explanatory notes in English and Hebrew). Scale 1 : 50,000. Geological Survey of Israel, Jerusalem.
- Begin, Z. B.; Ehrlich, A.; and Nathan, Y. 1974. Lake Lisan, the Pleistocene precursor of the Dead Sea. *Geol. Surv. Isr. Bull.* 63:1–30.
- Ben-Avraham, Z. 1997. Geophysical framework of the Dead Sea: structure and tectonics. *In* Niemi, T. M.; Ben-Avraham, Z.; and Gat, J. R., eds. *The Dead Sea: the lake and its settings*. Oxf. Monogr. Geol. Geophys. 36. New York, Oxford University Press, p. 22–35.
- Ben-Avraham, Z.; Niemi, T. M.; Neev, D.; Hall, K. J.; and Levy, Y. 1993. Distribution of Holocene sediments and neotectonics in the deep north basin of the Dead Sea. *Mar. Geol.* 113:219–231.
- Ben-Menahem, A.; Nur, A.; and Vered, M. 1976. Tectonics, seismicity and structure of the Afro-Eurasian junction: the breaking of an incoherent plate. *Phys. Earth Planet. Inter.* 12:1–50.
- Booth-Rea, G.; Azañón, J. M.; Azor, A.; and Garcia-Dueñas, V. 2004. Influence of strike-slip fault segmentation on drainage evolution and topography: a case study: the Palomares Fault Zone (southeastern Beltics, Spain). *J. Struct. Geol.* 25:1615–1632.
- Bowman, D. 1995. Active surface rupture on the northern Arava fault, the Dead Sea Rift. *Isr. J. Earth Sci.* 44: 51–59.
- Broecker, W. S.; Andree, M.; Wolfli, W.; Oeschger, H.; Bonani, G.; Kennett, J.; and Peteet, D. 1988. The chronology of the last deglaciation: implications to the cause of the Younger Dryas event. *Paleoceanography* 3:1–19.
- Ferry, M.; Meghraoui, M.; Karaki, N. A.; Al-Taj, M.; Amoush, H.; Al-Dhaisat, S.; and Barjous, M. 2007. A 48-kyr-long slip rate history for the Jordan Valley segment of the Dead Sea Fault. *Earth Planet. Sci. Lett.* 260:394–406.
- Freund, R.; Garfunkel, Z.; Zak, I.; Goldberg, M.; Weissbrod, T.; and Derin, B. 1970. The shear along the Dead Sea rift. *Philos. Trans. R. Soc. A* 267:107–130.
- Gardosh, M.; Reches, Z.; and Garfunkel, Z. 1990. Holocene tectonic deformation along the western margins of the Dead Sea. *Tectonophysics* 180:123–137.
- Garfunkel, Z. 1981. Internal structure of the Dead Sea

- leaky transform (rift) in relation to plate kinematics. *Tectonophysics* 80:81–108.
- Garfunkel, Z.; Zak, I.; and Freund, R. 1981. Active faulting in the Dead Sea rift. *Tectonophysics* 80:1–26.
- Goodfriend, G. A., and Magaritz, M. 1988. Paleosols and Late Pleistocene rainfall fluctuations in the Negev Desert. *Nature* 332:144–146.
- Hofstetter, R.; Klinger, Y.; Amrat, A. Q.; Rivera, L.; and Dorbath, L. 2007. Stress tensor and focal mechanisms along the Dead Sea fault and related structural elements based on seismological data. *Tectonophysics* 429:165–181.
- Joffe, S., and Garfunkel, Z. 1987. The plate kinematics of the circum Red Sea: a reevaluation. *Tectonophysics* 141:5–22.
- Kaufman, A.; Yechieli, Y.; and Gardosh, M. 1992. Reevaluation of lake sediment chronology in the Dead Sea basin, Israel, based on new  $^{230}\text{Th}/\text{U}$  dates. *Quat. Res.* 38:292–304.
- Klinger, Y.; Avouac, J. P.; Abou Karaki, N.; Dorbath, L.; Bourles, D.; and Reyss, J. L. 2000. Slip rate on the Dead Sea transform fault in northern Araba Valley (Jordan). *Geophys. J. Int.* 142:755–768.
- Lazar, M. 2004. Tectonic processes along the northern edges of pull-apart basins in the Dead Sea rift: a case study from the northern Dead Sea. PhD dissertation, Tel Aviv University.
- Lazar, M., and Ben-Avraham, Z. 2002. First images from the bottom of the Dead Sea: indications of recent tectonic activity. *Isr. J. Earth Sci.* 51:211–218.
- Lazar, M.; Ben-Avraham, Z.; and Schattner, U. 2006. Formation of sequential basin along a strike slip fault: geophysical observations from the Dead Sea basin. *Tectonophysics* 421:53–69.
- Mahmoud, S.; Reilinger, R.; McClusky, S.; Vernant, P.; and Tealeb, A. 2005. GPS evidence for northward motion of the Sinai Block: implications for E. Mediterranean tectonics. *Earth Planet. Sci. Lett.* 238:217–224.
- Marco, S., and Agnon, A. 1995. Prehistoric earthquake deformations near Masada, Dead Sea graben. *Geology* 23:695–698.
- Marco, S.; Agnon, A.; Ellenblum, R.; Eidelman, A.; Basson, U.; and Boas, A. 1997. 817-year-old walls offset sinistrally 2.1 m by the Dead Sea Transform, Israel. *J. Geodyn.* 24:11–20.
- Marco, S.; Rockwell, T. K.; Heimann, A.; Frieslander, U.; and Agnon, A. 2005. Late Holocene slip of the Dead Sea Transform revealed in 3D palaeoseismic trenches on the Jordan Gorge Fault. *Earth Planet. Sci. Lett.* 234:189–205.
- McCalpin, J. P. 1996. *Paleoseismology*. San Diego, CA, Academic Press, 588 pp.
- Neev, D., and Hall, J. K. 1979. Geophysical investigations of the Dead Sea. *Sediment. Geol.* 23:209–238.
- Pe'eri, S.; Wdowinski, S.; Shtibelman, A.; Bechor, N.; Bock, Y.; Nikolaidis, R.; and van Domselaar, M. 2002. Current plate motion across the Dead Sea fault from three years of continuous GPS monitoring. *Geophys. Res. Lett.* 29, 1697, doi:10.1029/2001GL013879.
- Quennell, A. M. 1959. Tectonics of the Dead Sea rift. *In Proc. 20th Int. Geol. Congr. Mex., 1956*, p. 385–403.
- Reches, Z., and Hoexter, D. F. 1981. Holocene seismic and tectonic activity in the Dead Sea Area. *Tectonophysics* 80:235–254.
- Reilinger, R.; McClusky, S.; Vernant, P.; Lawrence, S.; Ergintav, S.; Cakmak, R.; Ozener, H.; et al. 2006. GPS constraints on continental deformation in the Africa-Arabia-Eurasia continental collision zone and implications for the dynamics of plate interactions. *J. Geophys. Res.* 111:B05411, doi:10.1029/2005JB004051.
- Rotstein, Y.; Bartov, Y.; and Hofstetter, A. 1991. Active compressional tectonics in the Jericho area, Dead Sea Rift. *Tectonophysics* 198:239–259.
- Schramm, A.; Stein, M.; and Goldstein, S. L. 2000. Calibration of the  $^{14}\text{C}$  time scale to >40 ka by  $^{234}\text{U}/^{230}\text{Th}$  dating of Lake Lisan sediments (last glacial Dead Sea). *Earth Planet. Sci. Lett.* 175:27–40.
- Shamir, G. 2006. The active structure of the Dead Sea depression. *In Enzel, Y.; Agnon, A.; and Stein, M., eds. New frontiers in Dead Sea paleoenvironmental research. Geol. Soc. Am. Spec. Pap.* 401:15–32.
- Shamir, G.; Eyal, Y.; and Bruner, I. 2005. Localized versus distributed shear in transform plate boundary zones: the case of the Dead Sea Transform in the Jericho Valley. *Geochem. Geophys. Geosyst.* 6:1–21.
- Shapira, A. 1997. On the seismicity of the Dead Sea basin. *In Niemi, T. M.; Ben-Avraham, Z.; and Gat, J. R., eds. The Dead Sea: the lake and its settings. Oxf. Monogr. Geol. Geophys.* 36. New York, Oxford University Press, p. 82–86.
- Shapira, A.; Avni, R.; and Nur, A. 1993. A new estimate for the epicenter of the Jericho earthquake of 11 July 1927. *Isr. J. Earth Sci.* 42:93–96.
- Sieh, K. 1996. The repetition of large-earthquake ruptures. *Proc. Natl. Acad. Sci. USA* 93:3764–3771.
- Sneh, A.; Bartov, Y.; and Rosensaft, M. 1998. The geological map of Israel, sheet 2. Scale 1 : 200,000, 1 sheet. Jerusalem, Geological Survey of Israel.
- Somerville, P.; Saikia, C.; Wald, D.; and Graves, R. 1996. Implications of the Northridge earthquake for strong ground motions from thrust faults. *Bull. Seismol. Soc. Am.* 86:S115–S125.
- Stein, M. 2001. The sedimentary and geochemical record of Neogene-Quaternary water bodies in the Dead Sea basin: inferences for the regional paleoclimatic history. *J. Paleolimnol.* 26:271–282.
- Stuiver, M.; Reimer, P. J.; Bard, E.; Beck, J. W.; Burr, G. S.; Hughen, K. A.; Kromer, B.; McCormac, F. G.; van der Plicht, J.; and Spurk, M. 1998. INTCAL98 radiocarbon age calibration 24,000: 0 cal BP. *Radiocarbon* 40:1041–1083.
- Talebjan, M.; Fielding, E. J.; Funning, G. J.; Ghorashi, M.; Jackson, J.; Nazari, H.; Parsons, B.; et al. 2004. The 2003 Bam (Iran) earthquake: rupture of a blind strike-slip fault. *Geophys. Res. Lett.* 31:L11611.1–L11611.4.
- ten Brink, U.; Rybakov, M.; Al-Zoubi, A.; Hassouneh, M.; Batayneh, A.; Frieslander, U.; Goldschmit, V.; Daoud, M.; and Rotstein, Y. 1998. Bouguer gravity anomaly

- map of the Dead Sea fault system, Jordan and Israel. USGS Open-File Rep. 98-516.
- van Eck, T., and Hofstetter, A. 1990. Fault geometry and spatial clustering of microearthquakes along the Dead Sea-Jordan rift fault zone. *Tectonophysics* 180:15–27.
- Waldmann, N.; Starinsky, A.; and Stein, M. 2007. Primary carbonates and Ca-chloride brines as monitors of a paleo-hydrological regime in the Dead Sea basin. *Quat. Sci. Rev.* 26:2219–2228.
- Wdowski, S.; Bock, Y.; Baer, G.; Prawirodirdjo, L.; Bechor, N.; Naaman, S.; Knafo, R.; Forrai, Y.; and Melzer, Y. 2004. GPS measurements of current crustal movements along the Dead Sea Fault. *J. Geophys. Res.* 109: B05403, doi:10.1029/2003JB002640.
- Yeichieli, Y.; Magaritz, M.; Levy, Y.; Weber, U.; Kafri, U.; Woelfl, W.; and Bonani, G. 1993. Late Quaternary geological history of the Dead Sea area, Israel. *Quat. Res.* 39:59–67.
- Zak, I. 1967. The geology of Mt. Sedom. PhD dissertation, Hebrew University, Jerusalem.
- Zak, I., and Freund, R. 1966. Recent strike slip movements along the Dead Sea Rift. *Isr. J. Earth Sci.* 15:33–37.
- Zilberman, E.; Amit, R.; Porat, N.; Enzel, Y.; and Avner, U. 2005. Surface ruptures induced by the devastating 1068 AD earthquake in the southern Arava Valley, Dead Sea Rift, Israel. *Tectonophysics* 408:79–99.